

# Twocomponent Fermi vapour in a 2D rotating trap

Sankalpa Ghosh<sup>1</sup>, M.V.N.Murthy<sup>1</sup> and Subhasis Sinha<sup>2</sup>

*1. The Institute of Mathematical Sciences, Chennai 600113, India*

*2. Laboratoire Kastler-Brossel, Ecole Normale Supérieure, 24 rue Lhomond 75 231 Paris Cedex  
05. France*

## Abstract

An exactly solvable model of two-component interacting Fermi vapour in two dimension within Thomas Fermi approach has been proposed. We assume a realistic off-diagonal s-wave interaction between fermions in the two hyperfine states. The interaction is taken to be given by a screened Coulomb interaction which is both relevant and is analytically tractable. There are two distinct limits in the case of trapped fermionic systems: When the rotating frequency is less than the trap frequency a Thomas-Fermi approach may be used for a reasonably large number of particles. In the case of rapidly rotating fermions, an alternative variational approach is used, where the local density approximation may be applied after projecting the system on to the lowest degenerate level. Analytic expressions for the relevant physical quantities are obtained and their significance is discussed in both these cases.

## I. INTRODUCTION

The experimental observation of Bose-Einstein Condensation(BEC) in extremely cold dilute gas of atoms has generated a lot of activity both on experimental as well as theoretical fronts on the properties of trapped dilute gases near the quantum degeneracy limit. There is now a renewed focus on the properties of trapped dilute gas of fermionic atoms at low temperatures. Magneto-optical confinement of fermionic gases has been reported for  ${}^6\text{Li}$  [1] and  ${}^{40}\text{K}$  [2]. A recent significant success in this direction is the experimental observation of quantum degeneracy in a dilute gas of trapped fermionic atoms [3]. They have realised the magneto-optical trapping of  ${}^{40}\text{K}$  atoms in two different hyperfine states corresponding to  $|F = 9/2, m_F = 9/2 \rangle$  and  $|F = 9/2, m_F = 7/2 \rangle$  and finally reaching a single component Fermi vapour by selective removal of atoms in one of the hyperfine states. Amoruso *et.al.* [4] have studied the ground state and small amplitude excitations of such two component degenerate Fermi vapours placing them in spherically symmetric trap and discuss the effect of interaction on dissipative hydrodynamic processes in them. Salasnich *et.al.* [5] have studied the thermodynamic properties of such multicomponent fermi vapours theoretically and have pointed out that such systems can show phase separation and as well as shell effects.

While the effective interaction between  ${}^{40}\text{K}$  atoms in two different hyperfine states is repulsive a negative scattering length for  ${}^6\text{Li}$  atoms holds promise of achieving a superfluid state in a mixture of  ${}^6\text{Li}$  atoms prepared in two hyperfine states [6]. This has motivated a number of theoretical papers. Recently collective excitations of the system in the normal phase [8] and in the superfluid phase [9] have been investigated. Ghosh and Sinha [10] have studied [10] the low lying collective excitations of Fermi and Bose systems in an anisotropic trap.

Especially relevant to this paper is the recent interest in the properties of rotating bose condensates [11] and the experimental observation of vortices in stirred BEC of  ${}^{87}\text{Rb}$  [12]. The properties of ground and low excited states of a rotating and weakly interacting Bose-

Einstein condensate in a harmonic trap has been investigated recently in various limits [13–15]. Benakli *et.al.* [16] have studied the properties of macroscopic angular momentum state of a rotating BEC in a toroidal trap and identified  $l$ -dependent density profile as a signature of condensate rotation and superfluidity. Another very interesting theoretical issue related to the rotating BEC is the exact mapping of the problem in the limit of weak interaction to that of Lowest Landau Level problem in Quantum Hall effect [17]. Recently, experiments [7] has been able to trace a collective state of 160 vortices in a BEC consisting of  $Na$  atoms by imparting a large angular momentum to the system by rotating it. . This experiment is a major step towards realising this weakly interacting regime where the LLL mapping is useful. Theoretical model of such vortex lattice state has been discussed by Ho by invoking the fact that this system has a strong resemblance with the Quantum Hall systems.( [19]).

It is therefore quite natural to extend the analysis to Fermi vapours also. Ho and Ciobanu [18] have recently examined theoretically the nature the ground state of a rapidly rotating trapped Fermi gas in two and three dimensions in the noninteracting limit. They show that the density profile acquires features reflecting the underlying Landau level like energy spectrum when the frequency of rotation approaches the bare confinement frequency. Properties of the spectrum of such a system had been earlier investigated in detail by Bhaduri et al [20].

A simple and straight forward way of studying the ground state properties of such interacting many-body system is through the Thomas-Fermi(TF) approximation. Butts and Rokhsar [21] studied the momentum and spatial distribution of the noninteracting system and identify the region in which TF approximation is valid. The ground state properties and the addition energy spectra of a two-dimensional interacting Fermi system has been studied by Sinha et al [22] within Thomas Fermi approximation using an exactly solvable model interaction. A similar exactly solvable TF model has been discussed for a two dimensional parabolic quantum dot in a weak magnetic field by R. Pino ( [23]).

In this paper we analyse a multicomponent Fermi vapour confined in a rotating trap in

two dimension within the Thomas Fermi approximation and with an effective interaction between the fermions. If the confinement along the axis of rotation ( $z$ - axis) is relatively much stronger, then only a few lowest energy subbands along that direction get populated. In such a situation the system becomes effectively a multicomponent two dimensional Fermi gas, the number of components being the number of subbands being occupied. In particular when one uses optical traps such a system is experimentally realisable [24]. In the case of rotating Bose gas such two-dimensional systems have been extensively studied [15], but similar studies for their fermionic counterparts is still far from complete. The effective interaction is given by a screened Coulomb potential with a finite range. We show that within the TF approximation the system may be solved exactly and discuss the consequent results. We follow closely the formalism developed by Gallego and Das Gupta [25] who developed the TF method for the rotating nuclei. An attractive feature of the TF method is the ease with which non-trivial many-body solutions can be obtained even when they are interacting. As we have shown in a preceding work [26], in some cases the results may be obtained purely by analytical methods. In this paper we discuss a model interaction which is relevant to physical systems. Appropriate limits can reproduce the results already obtained in ref. [26]. Though our discussion is centered around rotating fermions in two dimension it is equally applicable to systems like quantum dot in a parabolic confinement with [23] or without a magnetic field [22].

The paper is organised as follows. In section II we outline the derivation of the Thomas Fermi energy functional for a system of interacting rotating fermions in parabolic confinement and discuss our choice of effective interaction. In section III we apply the formalism to a two-component Fermi gas when the rotational frequency is less than the confinement frequency and obtain analytic expressions for various quantities of physical interest. We also present numerical results for the interaction energy, the rotational energy and the spatial density in a given angular momentum sector for a given number of particles. Furthermore we discuss the extreme quantum limit where a rapidly rotating Fermi gas can be mapped exactly to the problem of a charged particle in uniform transverse magnetic field in 2 -

dimension. Exploiting this similarity we have analysed the many particle spectrum through a variational technique which is an improvement over the usual semiclassical method. The last section contains a discussion and summary of the results.

## II. THOMAS FERMI ENERGY FUNCTIONAL

We derive the Thomas-Fermi(TF) energy functional for a confined two dimensional rotating fermi gas starting from the microscopic Hamiltonian. We shall follow the approach outlined by Gallego and Das gupta [25] who derived the TF density functional for rotating nuclei, but applied to a two dimensional system.

The microscopic Hamiltonian of a two-dimensional rotating Fermi gas of  $N$  particles confined in a harmonic potential is given by,

$$H = \sum_{i=1}^N \frac{\mathbf{p}_i^2}{2m} + \sum_{i<j} V(\vec{r}_i, \vec{r}_j) + \sum \frac{1}{2} m \omega_0^2 r_i^2 - \sum m \omega [\mathbf{r}_i \times \mathbf{p}_i], \quad (1)$$

where  $V(\vec{r}_i, \vec{r}_j)$  denotes the two body interaction between fermions,  $\omega_0$  and  $\omega$  denote the confinement and rotational frequencies respectively.

We want to minimise the energy of this system subject to the constraints

$$\int d\vec{r} \rho(\vec{r}) = N, \quad (2)$$

$$\int d\vec{r} d\vec{p} f(\vec{r}, \vec{p}) (\vec{r} \times \vec{p}) = L, \quad (3)$$

where  $N$  and  $L$  are total particle number and the total Angular momentum,  $f(\vec{r}, \vec{p})$  is the semiclassical phase space density which we shall define later. The configuration space density  $\rho$  is obtained by integrating the phase space density over the momentum space.

Using Lagrange multiplier  $\mu$  and  $\omega$  for each constraint respectively and regrouping the momentum dependent term we obtain the following expression for the energy functional

$$E[\rho] = \int d\vec{r} d\vec{p} f(\vec{r}, \vec{p}) \left[ \frac{p^2}{2m} - \omega(xp_y - yp_x) \right] + \int d\vec{r} [V(\vec{r}) - \mu] \rho(\vec{r}) + \mu N + \omega L \quad (4)$$

where the mean-field one body interaction  $V(r)$  is

$$V(r) = \frac{1}{2}m\omega_0^2 r^2 + V_H(\vec{r}). \quad (5)$$

Note that the formalism itself is valid for arbitrary confinement potentials as long as the meanfield has a smooth behaviour. However in the later sections we restrict our analysis to parabolic confinement.

The Hartree term is given by,

$$V_H(\vec{r}) = \int d^2r V(\vec{r}, \vec{r}') \rho(\vec{r}'). \quad (6)$$

We ignore the exchange correction as it is in general subdominant compared to the Hartree term.

The semiclassical phase space density is given by

$$f(\vec{r}, \vec{p}) = \frac{2}{(2\pi\hbar)^2} \Theta(\mu - \epsilon(\vec{p}, \vec{r})), \quad (7)$$

where we have accounted for a factor of 2 due to spin degeneracy and

$$\epsilon(\vec{p}, \vec{r}) = \frac{p^2}{2m} + V(\vec{r}) - \omega(xp_y - yp_x) \quad (8)$$

denotes the energy density in phase space. We may rewrite this by completing the square as,

$$\epsilon(\vec{p}, \vec{r}) = \frac{1}{2m} [(p_x + m\omega y)^2 + (p_y - m\omega x)^2] + V(\vec{r}) - \frac{1}{2}m\omega^2 r^2. \quad (9)$$

The shifted momentum simply indicates that the center of the Fermi sphere at any given point  $\vec{r}$  in the rotating frame is displaced from the usual  $\vec{p} = 0$ . This shift is of no relevance within the classical TF approximation except for the appearance of the extra centrifugal term in the energy functional.

The TF energy functional is therefore given by,

$$E[\rho] = \int d^2r \left[ \frac{\pi\hbar^2 \rho^2}{2m} + \frac{1}{2}m\Omega r^2 + V_H - \mu \right] \rho(\vec{r}) + \mu N + \omega L \quad (10)$$

where

$$\Omega^2 = \omega_0^2 - \omega^2 \quad (11)$$

denotes the effective frequency in the presence of rotations. The TF equation for the spatial density is obtained by a variation of the energy functional, namely,

$$\frac{\pi\hbar^2\rho}{m} + \frac{1}{2}m\Omega^2r^2 + V_H = \mu \quad (12)$$

To obtain the ground state density in TF approximation one has to solve the above equation self-consistently with the boundary condition that the density vanishes beyond the classical turning point  $r_0$ , that is

$$\rho(r) = 0, \quad r \geq r_0. \quad (13)$$

Note that in the absence of rotations  $\Omega = \omega_0$  and the solution of the above equation describes the ground state in the absence of rotations which has been analysed in detail before [22]. We may remark that in general the above equation is difficult to solve analytically except in specific cases which we shall discuss later.

The angular momentum carried by the system is given by,

$$L = \int d^2r d^2p f(\vec{r}, \vec{p})(xp_y - yp_x) = m\omega \int d^2r \rho(\vec{r})r^2 \quad (14)$$

which is simply the classical expression for the angular momentum. We may therefore identify the Lagrange multiplier  $\omega$  with the angular frequency.

We may also define the related energy functionals. The free energy of the system is given by,

$$F = E - \mu N - \omega L \quad (15)$$

The TF equation (12) may also be obtained just by varying the free energy. We also define the energy in the rotating frame through

$$E = E' + \omega L, \quad (16)$$

where  $E$  is the total energy in the static frame. With the help of eq. (12) it can be shown that irrespective of the nature of the interaction  $E'$  is given by,

$$E' = \frac{1}{2}\mu N + \frac{1}{4}m\Omega^2 \int d^2r r^2 \rho. \quad (17)$$

Note that it is necessary that we choose  $\omega \leq \omega_0$  as otherwise the system becomes unstable.

This concludes the basic TF formalism applied to rotating fermionic systems. In the following section we solve the TF equation for a specific case. In an earlier brief note ([26]) we considered some examples of model interactions for which the TF equations are exactly solvable for a circularly symmetric density profile. In here we extend our calculation to the case of effective (screened) Coulomb interaction. Depending on the range (which is a free parameter in our calculation) the interaction yields both logarithmic as well as the contact interaction.

The Screened Coulomb interaction for a two dimensional system is given by

$$V(\vec{r}) = \frac{g}{2\pi} \int \frac{e^{i\vec{k}\cdot\vec{r}} d\vec{k}}{k^2 + \delta^2}, \quad (18)$$

where  $g$  is the coupling constant and the  $\delta$  denotes the relevant mass scale which determines the range of interaction. The choice of the effective interaction is dictated not only by the fact that it is tractable, but also by the fact that it is a good approximation to the realistic interaction between charged fermions in two dimensions. Given the very general form we have used in terms of the coupling constant  $g$  and the range  $b$  even for the neutral atomic (Fermi) vapours the consideration of such finite range interaction is quite important ([29]). It can be checked that the above integral can easily written as

$$V(r) = gK_0\left(\frac{r}{b}\right), \quad (19)$$

where  $K_0$  is the modified Bessel function and  $b = \frac{1}{\delta}$  denotes the range of the interaction.

When the range is very small then the given form of  $V(\vec{r})$  behaves almost like contact interaction and in the limit of  $b \rightarrow \infty$  the interaction goes over to the logarithmic interaction which is Coulomb interaction in an ideal two-dimensional system. These can be checked from the following limiting behaviour of the modified bessel function  $K_0(z)$  [28]:

$$b \rightarrow \infty \Rightarrow \frac{r}{b} \rightarrow 0,$$

$$K_0\left(\frac{r}{b}\right) \sim -\log\left(\frac{r}{b}\right) \quad (20)$$

and

$$b \rightarrow 0 \Rightarrow \frac{r}{b} \rightarrow \infty$$

$$K_0\left(\frac{r}{b}\right) \rightarrow 2\pi b^2 \delta^2(\vec{r}) \quad (21)$$

Hence in the two extreme limits we obtain the logarithmic and the contact like behaviour. In Fig. 1 we have plotted for comparisons three different potentials  $V(x)$  as a function of  $x$  - namely the Coulomb in two dimension  $1/x$ , the negative of logarithmic interaction  $-\log|x|$ , and the screened Coulomb  $K_0(x)$ . All distances are measured in units of length is defined by  $l_0 = \sqrt{\frac{\hbar}{m\omega_0}}$ . For the purpose of comparison we have set the range  $\tilde{b} = 1$ . It is easy to see that at long distance screened Coulomb falls faster than the unscreened Coulomb potential whereas at the short distance it goes like  $-\log|x|$ . We also note that for comparison we should only look at the portion of the plot of  $-\log|x|$  upto  $x = 1$  where the potential vanishes.

The TF analysis in these two limits has already been done in the previous paper [26]. In the following section we solve the TF equations for a general screened Coulomb interaction and discuss the results. The only approximation which has gone into obtaining the solutions is the assumption that the density is circularly symmetric.

### III. TWO-COMPONENT FERMI GAS WITH EFFECTIVE SCREENED COULOMB INTERACTION

For a two component system the coupling constant can be written in a  $2 \times 2$  matrix form to take care of inter and intra component interaction. We assume that such interaction strength matrix is symmetric in its off-diagonal components *i.e.*,  $g_{12} = g_{21} = g$ . Due to the anti-symmetry of the many body wave function the fermions occupying the same hyperfine state do not have the s-wave interaction but interact through the much weaker

p-wave interaction. To obtain the leading order results, we neglect this. Therefore we set  $g_{11} = g_{22} = 0$ .

The Thomas Fermi free energy functional of such two component Fermi vapour is therefore given by

$$F[\rho_1, \rho_2] = \int d\mathbf{r} \left[ \frac{\pi \hbar^2}{m} (\rho_1^2 + \rho_2^2) + \frac{1}{2} m \Omega^2 r^2 (\rho_1 + \rho_2) \right. \\ \left. + \rho_1(\vec{r}) \int d\mathbf{r}' V_{12}(|\vec{r} - \vec{r}'|) \rho_2(\vec{r}') \right] - \mu_1 N_1 - \mu_2 N_2, \quad (22)$$

where  $\rho_1, \rho_2$  denotes the densities of the two components while  $N_1$  and  $N_2$  denote the populations of the two hyperfine states which is kept fixed during minimisation. Furthermore, we have

$$V_{12}(|\vec{r} - \vec{r}'|) = \frac{g_{12}}{2\pi} \int \frac{e^{i\vec{k} \cdot (\vec{r} - \vec{r}')} d\vec{k}}{k^2 + \delta^2} \quad (23)$$

for the interaction matrix.

In what follows we use the dimensionless variables (denoted as variables with  $\tilde{\cdot}$  on top). The quantities with energy dimensions are measured in units of  $\hbar\omega_0$  and the length is measured in units of  $l_0 = \sqrt{\frac{\hbar}{m\omega_0}}$ . After this rescaling the free energy functional may be written as,

$$\tilde{F}[\tilde{\rho}_1, \tilde{\rho}_2] = \int d\tilde{x} \left[ \pi (\tilde{\rho}_1^2 + \tilde{\rho}_2^2) + \frac{\tilde{\Omega}^2 \tilde{x}^2 (\tilde{\rho}_1 + \tilde{\rho}_2)}{2} + \tilde{\rho}_1 \int d\tilde{x}' V_{12}(\tilde{x}, \tilde{x}') \tilde{\rho}_2(\tilde{x}') \right] - \tilde{\mu}_1 N_1 - \tilde{\mu}_2 N_2, \quad (24)$$

where scaled variables are given by

$$\begin{aligned} \tilde{\mu}_\alpha &= \frac{\mu_\alpha}{\hbar\omega_0} \\ \tilde{\Omega}^2 &= \frac{\Omega^2}{\omega_0^2} \\ \tilde{\rho}_\alpha &= \rho_\alpha l_0^2 \\ x &= \frac{r}{l_0} \end{aligned} \quad (25)$$

Minimising the free energy functional, we get the equations for the TF densities,

$$2\pi\tilde{\rho}_1 = \tilde{\mu}_1 - \tilde{V}_{H1} - \frac{1}{2}\tilde{\Omega}^2x^2, \quad (26)$$

$$2\pi\tilde{\rho}_2 = \tilde{\mu}_2 - \tilde{V}_{H2} - \frac{1}{2}\tilde{\Omega}^2x^2, \quad (27)$$

where

$$\tilde{V}_{H\alpha}(x) = \frac{1}{\hbar\omega_0} \int d\vec{x}' V_{\alpha\beta}(|\vec{x} - \vec{x}'|) \tilde{\rho}_\beta(\vec{x}') \quad (28)$$

By definition the Hartree potential obeys the following set of Poisson's equations,

$$\nabla^2 \tilde{V}_{H1} = -2\pi\tilde{g}\tilde{\rho}_2 + \frac{\tilde{V}_{H1}(x)}{\tilde{b}^2}, \quad (29)$$

and

$$\nabla^2 \tilde{V}_{H2} = -2\pi\tilde{g}\tilde{\rho}_1 + \frac{\tilde{V}_{H2}(x)}{\tilde{b}^2}, \quad (30)$$

where the coupling  $\tilde{g} = \frac{q}{\hbar\omega_0}$  and the range parameter is now given by  $\tilde{b} = \frac{b}{l_0}$  and,  $\tilde{\rho}_{1,2}$  is the density in dimensionless units ( $\tilde{\rho} = \rho(\vec{r})l_0^2$ )

Substituing Eqs. (29,30) in eqs. (26,27) we get following equations for the two densities,

$$2\pi\nabla^2\tilde{\rho}_1 + 2\tilde{\Omega}^2 - 2\pi\tilde{g}\tilde{\rho}_2 + \frac{1}{\tilde{b}^2}(\tilde{\mu}_1 - 2\pi\tilde{\rho}_1 - \frac{1}{2}x^2\tilde{\Omega}^2) = 0 \quad (31)$$

and

$$2\pi\nabla^2\tilde{\rho}_2 + 2\tilde{\Omega}^2 - 2\pi\tilde{g}\tilde{\rho}_1 + \frac{1}{\tilde{b}^2}(\tilde{\mu}_2 - 2\pi\tilde{\rho}_2 - \frac{1}{2}x^2\tilde{\Omega}^2) = 0. \quad (32)$$

The eqs. (31) and (32) may be solved subject to the usual boundary conditions

$$\tilde{\rho}_1 = 0 \text{ at } x \geq x_1 \quad (33)$$

$$\tilde{\rho}_2 = 0 \text{ at } x \geq x_2 \quad (34)$$

At this stage it is useful to define the following quantities

$$\tilde{\rho} = \tilde{\rho}_1 + \tilde{\rho}_2, \quad (35)$$

$$\tilde{s} = \tilde{\rho}_1 - \tilde{\rho}_2, \quad (36)$$

$$\tilde{\mu}^\pm = (\tilde{\mu}_1 \pm \tilde{\mu}_2), \quad (37)$$

where  $\tilde{\rho}$  denotes the total density, and  $\tilde{s}$  denotes the spin density. It is easy to see that in terms of the density and the spin density the coupled equations for the two components are diagonal. In this paper we consider the case when the system is unpolarised, that is when the spin density is zero. The case of partially polarised system will be discussed in detail in a forthcoming publication [27].

Before proceeding further we note that, since  $\Omega^2 = \omega_0^2 - \omega^2$ , the system becomes unstable when the rotational frequency approaches the confinement frequency. TF method can be applied abinitio only to the case when the rotational frequency is less than the confinement frequency. In the rapidly rotating case many levels collapse into the lowest one reminding one of the Lowest Landau Level (LLL) structure. We discuss these two cases separately in what follows.

### A. Trapped rotating fermions

When the particle number in the two hyperfine states are equal the system is unpolarized. Since the interaction strength is symmetric, the turning points are therefore the same. This situation changes only if there is a spontaneously broken symmetry in the ground state leading towards phase separation.

For the unpolarised case the spin density  $\tilde{s}(\vec{x})$  vanishes everywhere. Adding eqs.(31) and (32) we obtain

$$2\pi\nabla^2\tilde{\rho} + 4\tilde{\Omega}^2 - 2\pi\tilde{g}\tilde{\rho} + \frac{1}{\tilde{b}^2}(\tilde{\mu}^+ - 2\pi\tilde{\rho} - x^2\tilde{\Omega}^2) = 0 \quad (38)$$

The same equation may also be obtained by minimising the energy functional given in the previous section, see eq.(10) where we simply considered a system with spin degeneracy of 2 as in the unpolarised case.

The solution of the above equation may be written in terms of the modified Bessel function, namely

$$2\pi\tilde{\rho} = AI_0(\eta x) + \frac{1}{\eta^2\tilde{b}^2}[\tilde{\mu}^+ + \frac{4\tilde{\Omega}^2\tilde{b}^2\tilde{g}}{\eta^2} - x^2\tilde{\Omega}^2], \quad (39)$$

where

$$\eta^2 = (\tilde{g} + \frac{1}{\tilde{b}^2}) \quad (40)$$

The solution for the density has three unknown parameters, the turning point  $x_0$ , the overall normalisation  $A$  and the chemical potential  $\tilde{\mu}^+$ . In the following we outline how these may be determined from the known constraints. The first constraint arises from the fact that at the classical turning point the density vanishes. We may use this condition to determine the chemical potential:

$$\tilde{\mu}^+ = -\tilde{b}^2 \eta^2 A I_0(\eta x_0) + \tilde{\Omega}^2 x_0^2 - \frac{4\tilde{g}\tilde{\Omega}^2 \tilde{b}^2}{\eta^2} \quad (41)$$

This gives  $\tilde{\mu}^+$  in terms of the other two unknowns  $A$  and  $x_0$ . Substituting this we get

$$2\pi\tilde{\rho} = A I_0(\eta x_0) \left[ \frac{I_0(\eta x)}{I_0(\eta x_0)} - 1 \right] + \frac{\tilde{\Omega}^2}{\tilde{b}^2 \eta^2} [x_0^2 - x^2] \quad (42)$$

Interestingly, the first term in the above expression corresponds to the density obtained in the case of logarithmic interaction and the second term corresponds to the density obtained in the case of contact interaction if the coefficients are properly adjusted. These different limits were derived earlier in Ref. [26] separately for these two interactions.

The second constraint is given by the continuity of the Hartree potential and its derivative which is the electric field experienced by the charge distribution at the turning point. Adding eq. (29) and eq. (30) we have

$$\nabla^2 \tilde{V}_{H+} = -2\pi\tilde{g}\tilde{\rho} + \frac{\tilde{V}_{H+}}{\tilde{b}^2}, \quad (43)$$

where  $\tilde{V}_{H+}$  corresponds to the Hartree potential with

$$\tilde{V}_{H+} = \tilde{V}_{H1} + \tilde{V}_{H2}$$

In the region  $x \geq x_0$  the equation (43) takes the form

$$\nabla^2 \tilde{V}_{H+} = \frac{\tilde{V}_{H+}}{\tilde{b}^2} \quad (44)$$

since the density is zero beyond the turning point. The solution is given by

$$\tilde{V}_{H+} = \frac{A_1 K_0(x/\tilde{b})}{\tilde{b}^2}, \quad (45)$$

where  $A_1$  is an overall normalisation which is not needed in what follows. The electric field is just the negative of the gradient of this potential  $\mathbf{E} = -\nabla V$ . We define the ratio of the potential to the field as follows

$$\frac{\tilde{V}_{H+}(x_0)}{\mathbf{E}(x_0)} = \tilde{b} K_0(x_0/b')/K_1(x_0/b') \quad (46)$$

From eq. (26) and (27) we have for  $x \leq x_0$

$$\tilde{V}_{H+} = \tilde{\mu}_+ - \tilde{\Omega}^2 x^2 - \tilde{\rho} \quad (47)$$

Again taking the ratio of the potential and the electric field we have

$$\frac{\tilde{V}_{H+}(x_0)}{\mathbf{E}(x_0)} = -\frac{\mu - \Omega^2 x_0^2 - \tilde{\rho}(x_0)}{2\Omega^2 x_0 + (\tilde{\rho}(x))'|_{x=x_0}} \quad (48)$$

Now demanding the continuity of the potential and the field across the turning point we have from eqs.(46) and (48)

$$AI_0(\eta x_0) = -\frac{2\tilde{\Omega}^2 \tilde{g} \tilde{b}^2}{\eta^2} \frac{(2 + \frac{x_0 K_0(x_0/\tilde{b})}{\tilde{b} K_1(x_0/\tilde{b})})}{(\tilde{b}^2 \eta^2 + \tilde{b} \eta [\frac{(I_1(\eta x_0) K_0(\frac{x_0}{\tilde{b}}))}{I_0(\eta x_0) K_1(\frac{x_0}{\tilde{b}})])} \quad (49)$$

which now gives the relation between  $A$  and the turning point. Finally the turning point, and hence all the undetermined parameters are determined using the fact that the number of particles in the system is fixed. That is,

$$N = AI_0(\eta x_0) \left[ \frac{x_0 I_1(\eta x_0)}{\eta I_0(\eta x_0)} - \frac{x_0^2}{2} \right] + \frac{1}{4} \frac{\tilde{\Omega}^2 x_0^4}{\tilde{b}^2 \eta^2} \quad (50)$$

Note that the turning point increases with  $N$  in a nonlinear fashion given by the above relation. For large number of particles, however, the turning point is given by the following asymptotic relation

$$N \approx \frac{1}{4} \frac{\tilde{\Omega}^2 x_0^4}{\tilde{b}^2 \eta^2} \quad (51)$$

All the other relevant quantities defining the system may now be written down. The exact expression for the total angular momentum is given by

$$\frac{L}{\hbar} = AI_0(\eta x_0) \frac{\omega}{\omega_0} \left[ \left( \frac{x_0}{\eta} (x_0^2 + \frac{4}{\eta^2}) \frac{I_1(\eta x_0)}{I_0(\eta x_0)} - \frac{2x_0^2}{\eta^2} - \frac{x_0^4}{4} \right) + \frac{\omega}{\omega_0} \frac{\tilde{\Omega}^2}{\tilde{b}^2 \eta^2} \frac{x_0^6}{12} \right] \quad (52)$$

The Energy is again given by the expression

$$\frac{E}{\hbar \omega_0} = \frac{\tilde{\mu}^+ N}{2} + \frac{1}{4} \frac{\omega_0^2 - \omega^2}{\omega \omega_0} \frac{L}{\hbar} \quad (53)$$

It is easy to see that all the above expressions above can be written as a sum of contributions coming from the purely contact interaction and the purely logarithmic term ([26]), two extreme limits of the screened Coulomb interactions. However this is not valid for the interaction energy since it is bilinear in the density. This may be seen from the analytic expression for the interaction energy

$$\begin{aligned} \frac{E_{int}}{\hbar \omega_0} &= \frac{E}{\hbar \omega_0} - \pi^2 \int \tilde{\rho}^2 x dx - \frac{1}{2} \frac{\tilde{\Omega}^2 \omega_0}{\omega} \frac{L}{\hbar} \\ &= \frac{E}{\hbar \omega} - \frac{1}{4} (I_1 + I_2 + I_3) - \frac{1}{2} \frac{\tilde{\Omega}^2 \omega_0}{\omega} \frac{L}{\hbar}, \end{aligned} \quad (54)$$

where

$$I_1 = \left[ (AI_0(\eta x_0))^2 \left[ \frac{x_0^2}{2} \left[ 1 - \frac{I_1^2(\eta x_0)}{I_0^2(\eta x_0)} \right] - 2x_0 \frac{I_1(\eta x_0)}{I_0(\eta x_0)} + \frac{x_0^2}{2} \right] \right] \quad (55)$$

$$I_2 = AI_0(\eta x_0) \frac{\tilde{\Omega}^2}{\tilde{b}^2 \eta^2} \left[ 2 \frac{x_0^2}{\eta^2} \left[ 1 - \frac{2}{x_0 \eta} \frac{I_1(\eta x_0)}{I_0(\eta x_0)} - \frac{x_0^2 \eta^2}{8} \right] \right] \quad (56)$$

$$I_3 = \frac{1}{4} \left( \frac{\tilde{\Omega}}{\tilde{b} \eta} \right)^4 \frac{x_0^6}{6} \quad (57)$$

While the system is analytically solvable as shown above, the actual behaviour is not often easy to see. We illustrate the results for reasonably large systems with number of particles  $N = 50, 100, 1000$ . The numerical calculation is done in two different scenarios. In the first case we have kept the particle number  $N$ , the range  $\tilde{b}$  and coupling strength  $\tilde{g}$  fixed and vary the external frequency of rotation. In the second case we have calculated the relevant quantities as a function of the quantity  $\tilde{g}\tilde{b}^2$  where all the other quantities except the range  $\tilde{b}$  are kept fixed.

In Fig.2 we show the turning point  $x_0$  as a function of the frequency  $\omega$  measured in units of  $\omega_0$ . Note that Eq.(50) is highly nonlinear. In order to estimate the turning point we use the value given by the asymptotic result as an upperbound and use this value to iterate the exact equation to obtain the exact value of  $x_0$ . It is easy to see that the system size increases with rotational frequency. All other quantities are determined once the turning point is known. The system size increases with rotational frequency rather slowly as expected. The size variation with respect to the number of particles is approximately given by the asymptotic formula.

The angular momentum per particle also follows a similar behaviour. as shown in Fig. 3. The ratio of the energy of the system measured in terms of the ground state energy is shown in Fig.4. Shown also in this figure is the interaction energy for  $N = 1000$ . At low frequencies the interaction contributes substantially to the total energy. However, at large frequencies the interaction contributes little, and most of the total energy is simply the energy of rotation which is proportional to the angular momentum  $L$ . Following the analogy with rotating nuclei, this is usually referred to as the Yrast region [30] and has been a subject of intense study in recent times [13].

As already pointed out, the screened Coulomb interaction can mimic different types of two body interaction depending on the range. We study the system for  $N = 1000$  at a fixed frequency of  $\omega = 0.25\omega_0$ , in Figs. 5,6,7 where we have plotted the turning point, the angular momentum per particle and the total energy respectively as a function of  $\tilde{g}\tilde{b}^2$ . The quantity  $\tilde{g}\tilde{b}^2$  here is analogous to the coupling strength in the pseudopotential of a three dimensional Bose condensate,  $g_{3D} = \frac{4\pi\hbar^2 a}{m}$ , where  $a$  is the s-wave scattering length. Note that the system of fermions, for these purposes, may be regarded as a hardcore bosons. This three dimensional coupling constant is related to the two dimensional coupling constant by the formula ([15])  $g_{2D} = g_{3D}\sqrt{\frac{m\omega_z}{\hbar}}$ . We have estimated this constant using the parameters for  $^{40}\text{K}$  and chosen the appropriate range of  $\tilde{g}\tilde{b}^2$  (see ref. [10] for such an estimate). From these figures, it is easy to see that within the Thomas Fermi approximation the effect of change of range is considerable even at moderate rotational frequency as above. In particular

in Fig.7, we see that both the total and interaction energy increase with the range.

It should be mentioned that the analysis can also be extended to the partially polarised system where the number of particles in different components are not same . Formally one can write the solutions in closed form which however are more difficult to evaluate since the turning point for each component density will be different. This case will be considered in detail in another paper [27].

### B. Rapidly Rotating fermions

The above TF analysis is valid when the trapping frequency is larger than the rotational frequency. The effect of rotations is to reduce the effective trapping frequency and in the absence of interactions this leads to bunching of single particle levels. There are thus many similarities between the system of rotating fermions and the fermions in the presence of an external magnetic field along z-direction. The rotation frequency to plays a role analogous to the cyclotron frequency. We exploit this similarity in what follows.

Noninteracting Hamiltonian for a rapidly rotating system is given by,

$$H_0 = \sum_i \frac{\hat{p}_i^2}{2m} + \frac{1}{2}m\omega_0^2 r_i^2 - \omega \hat{L}_i, \quad (58)$$

where as before  $\omega$  is the external rotation frequency. The single particle energy levels are given by,

$$E_{n,l} = (2n + |l| + 1)\hbar\omega_0 - \hbar\omega l, \quad (59)$$

where  $n$  is the radial quantum number. This spectra is the same as that of a cranked harmonic oscillator with two frequencies  $\omega_0 + \omega$  and  $\omega_0 - \omega$  (for details see Ref. [20]). The Landau level like structure starts to form when  $(\omega_0 - \omega) \ll (\omega_0 + \omega)$  and the mixing between the different levels is suppressed. In particular when  $\omega_0 - \omega = 0$ , the spectrum becomes identical to that of a set of highly degenerate discrete Landau levels. In the other limit when the external rotation frequency is not too high and  $\mu \gg (\omega_0 + \omega)$ , so that many levels are occupied, the system is described by Thomas-Fermi approximation.

In the lowest Landau level (LLL) the particles have the radial quantum number  $n = 0$  and the angular momentum  $l \geq 0$ . The single particle wave functions and energies in LLL are given by,

$$\psi_l = \frac{1}{\sqrt{\pi l_0^2 l!}} \left(\frac{z}{l_0}\right)^l e^{-r^2/2l_0^2}, \quad (60)$$

$$E_l = (\omega_0 - \omega)\hbar l + \hbar\omega_0, \quad (61)$$

where  $l_0^2 = \frac{\hbar}{m\omega_0}$ , and  $z = x + iy$ .

The density of the non-interacting spin polarised electrons is given by,

$$\rho_0 = \frac{1}{\pi l_0^2} \sum_{l=0}^N \frac{1}{l!} (z/l_0)^l e^{-r^2/l_0^2}, \quad (62)$$

$$\approx \frac{1}{\pi l_0^2} \theta(R - r), \quad (63)$$

where,  $R$  is the radius of the system for large number of particles. In this limit the particles form a flat droplet like state.

We now consider the interacting two component unpolarised fermions in the “lowest Landau band” when the rotation frequency is almost equal to the external trap frequency. The interaction is taken to be the screened Coulomb interaction defined earlier. Since TF method can not be applied directly, we use the standard variational method for determining the ground state properties. We construct a local density functional by taking the expectation value of the quantum mechanical many particle Hamiltonian with the variational state given above, neglecting the mixing between the ground and excited states. The beauty of this method is that all quantities of physical interest may be derived analytically. Though this method also does not go beyond the mean field approximation, it performs better compared to the bare TF method since the variational ansatz does account for quantum mechanical effects.

The many body variational wave function for each component may be written as,

$$\psi(\{z_i\}) = f(\{z_i\}) e^{-\sum_i z_i \bar{z}_i / 2l_0^2}. \quad (64)$$

Kinetic energy of the system is then given by,

$$\langle T \rangle = \langle \psi | -\frac{\hbar^2}{2m} \left( 4 \frac{\partial}{\partial \bar{z}} \frac{\partial}{\partial z} \right) | \psi \rangle = \frac{1}{2} m \omega_0^2 \int r^2 \rho(r) d^2 r. \quad (65)$$

Note that the kinetic energy density is linear in  $\rho$ , that is,  $T[\rho] = \frac{1}{2} m \omega_0^2 r^2 \rho(r)$ , where as in the standard TF case it is quadratic. The total angular momentum of the two-dimensional system is given by,

$$\langle L \rangle = -\hbar \int [\psi^* \bar{z} \frac{\partial \psi}{\partial \bar{z}} - \frac{\partial \psi^*}{\partial z} z \psi] - \hbar \int \psi^* \psi = \int d^2 r [m \omega_0 r^2 - \hbar] \rho(r). \quad (66)$$

Using these, the energy density functional of two component fermi gas can be written as,

$$E[\rho_1, \rho_2] = T[\rho_1] + T[\rho_2] + V[\rho_1] + V[\rho_2] - \Omega(L[\rho_1] + L[\rho_2]) + E_{int}[\rho_1, \rho_2]. \quad (67)$$

This energy functional is similar to the magnetic field Thomas Fermi method developed by Lieb et al [33]. For the unpolarised system,  $\rho_1 = \rho_2$ . The free energy of the system may be written in terms of  $\rho = \rho_1 + \rho_2$  alone. Using the expression for kinetic energy density and scaling to dimensionless variables as before, the free energy of the two component system is given by

$$\frac{F[\rho]}{\hbar \omega_0} = (1 - \tilde{\omega}) \int d^2 x x^2 \tilde{\rho} + \frac{1}{4} \int d^2 x_1 d^2 x_2 \tilde{\rho}(x_1) \tilde{V}_{12}(|\vec{x}_1 - \vec{x}_2|) \tilde{\rho}(x_2) - (\tilde{\mu} - \tilde{\omega}) \int d^2 x \tilde{\rho}, \quad (68)$$

where  $\tilde{\omega} = \frac{\omega}{\omega_0}$ .

Minimising the free energy for a fixed number of particles gives the following integral equation for the density:

$$(1 - \tilde{\omega}) x^2 + \frac{1}{2} \int d^2 x' \tilde{V}_{12}(|\vec{x} - \vec{x}'|) \rho(x') = (\tilde{\mu} - \tilde{\omega}), \quad (69)$$

As noted before, the screened Coulomb potential satisfies, the following differential equation,

$$\nabla^2 \tilde{V}_H = -2\pi \tilde{g} \tilde{\rho} + \frac{\tilde{V}_H}{\tilde{b}^2}. \quad (70)$$

While the equation system looks complicated, the solution for the circularly symmetric case is rather simple and is given by,

$$\rho = \frac{\alpha}{\pi}(\tilde{\mu}_c - x^2), \quad (71)$$

where

$$\alpha = \frac{1 - \tilde{\omega}}{\tilde{g}\tilde{b}^2}, \quad (72)$$

$$\tilde{\mu}_c = \frac{\tilde{\mu} - \tilde{\omega}}{1 - \tilde{\omega}} + 4\tilde{b}^2. \quad (73)$$

One can easily recognise that the solution bears a resemblance to that of the lowest Landau level droplet for the rapidly rotating fermions.

The size of the droplet ( $R$ ) may be obtained by normalising the above density to yield the total number of particles  $N$  which is fixed. We have

$$\begin{aligned} \tilde{\mu}_c &= R^2 \\ R &= (2N/\alpha)^{1/4}. \end{aligned} \quad (74)$$

Now we are in a position to compute all quantities of interest relevant to the rapidly rotating two-component system. Angular momentum of the system is given by

$$L = \frac{\langle L \rangle}{\hbar} = \frac{1}{6}\alpha(2N/\alpha)^{3/2} - N. \quad (75)$$

For a given angular momentum this equation determines the parameter  $\alpha$  in terms of the fixed parameters  $L$  and  $N$ . That is,

$$\alpha = \frac{2}{9} \frac{N^3}{(L + N)^2}. \quad (76)$$

The interaction energy is then given by,

$$E_{int}(L, N, \tilde{g}, \tilde{b}^2) = \frac{2}{9} \frac{N^3 \tilde{g} \tilde{b}^2}{(L + N)^2} [L + N(1 - 2\tilde{b}^2)]. \quad (77)$$

The total energy in the rotating frame is given by,

$$\begin{aligned} E(L, N, \tilde{g}, \tilde{b}^2) &= (1 - \tilde{\omega}) \int d^2x x^2 \tilde{\rho} + \tilde{\omega} \int d^2x \tilde{\rho} + E_{int} \\ &= N + \frac{2}{9} \frac{N^3 \tilde{g} \tilde{b}^2}{(L + N)^2} [2L + N(1 - 2\tilde{b}^2)] \end{aligned} \quad (78)$$

Variation of the total energy with external rotation frequency is given by,

$$E(\tilde{\omega}, N, \tilde{g}, \tilde{b}^2) = N + \sqrt{\tilde{g}\tilde{b}^2(1 - \tilde{\omega})}(2N)^{3/2} - (1 - \tilde{\omega})N(1 + 2\tilde{b}^2). \quad (79)$$

Since  $\alpha \propto (1 - \tilde{\omega})$ , the angular momentum increases as the rotational frequency approaches the confinement frequency. In fact when  $\omega = \omega_0$ , the total angular momentum blows up, and the system resembles the LLL droplet. The total energy is given entirely by the energy of non-interacting LLL system since the interaction goes to zero. Total energy goes to the zero point energy as  $\sim \sqrt{1 - \tilde{\omega}}$ .

#### IV. SUMMARY

We have discussed a Thomas-Fermi model for a rotating two-component interacting Fermi vapour in two dimensions. We believe that the interaction, the screened Coulomb, is realistic with interesting limits as the range is varied. The results corresponding to short range and logarithmic interactions may be obtained with suitable approximations. More importantly the system is analytically solvable within the TF mean field approach. We have neglected the diagonal component of the interaction including the dominant s-wave off diagonal interaction. We have first considered the case when the trap frequency is larger than the rotational frequency since one can use the TF method ab initio. However when the rotational frequency is much larger than the trap frequency we first projected the system on to the lowest degenerate level and used a TF like approach to derive the analytical result. It should be noted that, in general, it is rather hard and near impossible to obtain accurate results for large number of particles using exact diagonalisation. In contrast, the TF method is solvable in a realistic case as shown and provides a reasonably good approximation. An important drawback in the present analysis is that we have not included the exchange corrections. This however is obviated if the number of particles in the system is large and sufficiently dilute.

To put the utility of the method in perspective, unlike in the case of superfluid bosons, the system of fermions has a rigid body rotation. A direct measurement of the angular

momentum in a system of bosons is very difficult. But in the case of fermions total angular momentum can be estimated just from a measurement of the moment of inertia. It is valid for low rotation frequencies, where the usual TF method is good. The radius of the cloud can be measured easily by observing the diffusion of the gas (by switching off the trap potential). In the rapidly rotating case, however, the total angular momentum is not proportional to  $\langle r^2 \rangle$  due to the quantum effects being large and a direct measurement of the angular momentum would be difficult. The system is however more interesting because of its similarity to the LLL problem. It would be interesting to see if the system exhibits quasiparticle (quasi hole )like excitations which is similar to the vortex excitations in the corresponding Bose systems.

One of us (S.S) acknowledge financial support from Ministère de la Recherche et de la Technologie. LKB is a unité de recherche de l'Ecole normale supérieure et de l'Université Pierre et Marie Curie, associée au CNRS.

## REFERENCES

- [1] W. I. McAlexander *et. al.* Phys. Rev. A. **51**, R871 (1995)
- [2] F. S. Cataliotti . *et. al.* Phys. Rev. A **57**, 1136 (1998)
- [3] B.Demarco and D. S. Jin, Science, **285**, 1703 (1999)
- [4] M. Amoruso, I Meccoli, A Minguzzi and M. P.Tosi , Eur. Phys. J. D **8**, 361 (2000)
- [5] L. Salasnich, B. Pozz, A. Parola and L. Reatto, J. Phys. B: At. Mol. Opt. Phys. **33**, 3943 (2000),L. Salasnich *et. al.* cond-mat/0011049
- [6] M Houbiers, R. Ferweda, H. T. C. Stoof, W. I. McAlexander, C.A. Sackett, R. G. Hulet Phys. Rev. A **56**, 4864 (1997)
- [7] J. R. Abo-Shaeer, C. Raman, J. M. Vogels, W. Ketterle , Science, **292**, 476
- [8] G. M. Brunn and C. W. Clark, Phys. Rev. Lett. **83** 5415 (1999)
- [9] M. A. Baranov and D. S. Petrov, Phys. Rev. A **62** 041601(R) (2000)
- [10] Tarun Kanti Ghosh and Subhasis Sinha e-print cond-mat/0102258
- [11] D. A. Butts and D. S. Rokhsar, Nature **397**,327 (1999)
- [12] K. W. Madison, F. Chevy, W. Wohlleben and J. Dallibard, Phys. Rev. Lett. **84**,806 (2000)
- [13] B. Mottelson Phys. Rev. Lett. **83**,2695 (1999)
- [14] G. M. Kavoulakis, B. Mottelson and C. J. Pethick, cond-mat/0004307; A. D. Jackson, G. M. Kavoulakis, B. Mottelson and S. M. Reimann, cond-mat/0004309
- [15] Y. Castin and R. Dum Eur. Phys. J. D **7**,399 (1999).
- [16] M Benakli, S. Raghavan, A. Smerzi, S Fantoni and S. R. Shenoy Euro. Phys. Lett, **46**,275 (1999)

- [17] N. K. Wilkin, J. M. F. Gunn, and R. A. Smith, Phys. Rev. Lett **80**, 2265 (1998), *ibid* Phys. Rev. Lett **84**,6 (2000), S. Viefers, T. H. Hansson and S. M Riemann Phys. Rev. A **62**, 053604 (2000)
- [18] T.L.Ho and C. V. Ciobanu, Phys. Rev. Lett **85**,4648 (2000)
- [19] T. L. Ho, Preprint cond-mat / 0104522
- [20] R. K. Bhaduri, S. Li, K. Tanaka and J. C. Waddington, J. Phys. A **27**, L553 (1994)
- [21] D. A. Butts and D. S. Rokhsar, Phys. Rev. A **55**, 4346 (1997)
- [22] Subhasis Sinha, R. Shankar, and M.V.N. Murthy, Phys. Rev. B **62**,10896 (2000)
- [23] R. Pino, Eur. Phys. J. B **13**, 723 (2000)
- [24] D. M. Stamper-Kurn, M. R. Andrews, A. P. Chikkatur, S. Inouye. H. -J. Miesner, J. Stenger, W. Ketterle Phys. Rev. Lett **80**,2027 (1998)
- [25] J. Gallego and S. Das Gupta, Phys. Lett. B **270**, 6 (1991).
- [26] Sankalpa Ghosh, M.V.N. Murthy and Subhasis Sinha, Preprint cond-mat/0011313 (*presented at SCES-Y2K, Calcutta, 2000*) ,in print.
- [27] Sankalpa Ghosh, M. V. N. Murthy and Subhasis Sinha (*in preparation*)
- [28] *Handbook of Mathematical Functions* ed. by M. Abramowitz and I.A. Stegun,(Dover Publication, New York),1970
- [29] Maxim Olshanii and Ludovic Pricoupenko, Preprint cond-mat/0101275
- [30] A. Bohr and B. R. Mottelson, *Nuclear Structure*,Vol. 2, (N. A. benjamin Inc., 1975)
- [31] R. K. Bhaduri, M. V. N. Murthy and M. K. Srivastava, Phys. Rev. Lett. **76**, 165(1996)
- [32] R. K. Bhaduri, S. Das Gupta and S. J. Lee, Am. J. Phys. **58**,983 (1990)
- [33] E.H. Lieb, J.P. Solovej and J. Yngvason, Phys. Rev. B **51**, 10646 (1995).

## FIGURES

FIG. 1. The spatial variation of three type of potentials namely  $\frac{1}{x}$  (dashed),  $-\log|x|$  (dotted) and the screened Coulomb  $K_0(x)$  (solid line)(where we have set  $\tilde{b} = 1$ ) is shown.

FIG. 2. The plot of turning point of the rotating fermions  $x_0$  as a function of the external frequency  $\omega$ . The unit of  $\omega$  is the confinement frequency  $\omega_0$  and the unit of length is  $l_0 = \sqrt{\frac{\hbar}{m\omega_0}}$ . The three curves correspond to  $N = 50$  (solid line),  $N = 100$  (short-dashed) and  $N = 1000$  (long-dashed). For all the curves plotted we have chosen  $\tilde{b} = 0.15$  and  $\tilde{g} = 0.1$ .

FIG. 3. The plot of angular momentum per particle of the rotating fermions  $L/N$  as a function of the external frequency  $\omega$ . The unit of  $\omega$  is the confinement frequency  $\omega_0$  and the unit of  $L$  is  $\hbar$ . The three curves correspond to  $N = 50$  (solid line),  $N = 100$  (short-dashed) and  $N = 1000$  (long-dashed). Again for all the curves plotted  $\tilde{b} = 0.15$  and  $\tilde{g} = 0.1$ .

FIG. 4. The plot of energy of the rotating fermions as a function of external frequency  $\omega$ . The unit of  $\omega$  is same as that in Fig.3. The energies are normalised to the  $\omega = 0$  case. The upper curve with dashed line shows the variation of the total energy and the lower curve (solid line) shows the variation of the interaction energy. The number of particles is  $N = 1000$  and  $\tilde{b} = 0.15$ ,  $\tilde{g} = 0.1$

FIG. 5. The plot of the turning point of the rotating fermions as a function of  $\tilde{g}\tilde{b}^2$  when  $\tilde{b}$  is varied. The number of particles  $N$ ,  $\tilde{g}$  and the frequency  $\omega$  (in units of  $\omega_0$ ) are respectively given by 1000, 0.1, 0.25.

FIG. 6. The plot of angular momentum per particle  $L/N$  as a function of  $\tilde{g}\tilde{b}^2$  when  $\tilde{b}$  is varied. The unit of angular momentum and length is again  $\hbar$  and  $l_0$  respectively. The number of particles  $N$ ,  $\tilde{g}$  and the frequency  $\omega$  (in units of  $\omega_0$ ) are respectively set at 1000, 0.1, 0.25.

FIG. 7. The plot of energy as a function of  $\tilde{g}\tilde{b}^2$  when  $\tilde{b}$  is varied. The continuous curve corresponds to the total energy where the dashed curve corresponds to the interaction energy alone. The number of particles  $N$ ,  $\tilde{g}$  and the frequency  $\omega$  (in units of  $\omega_0$ ) are given by 1000, 0.1, 0.25

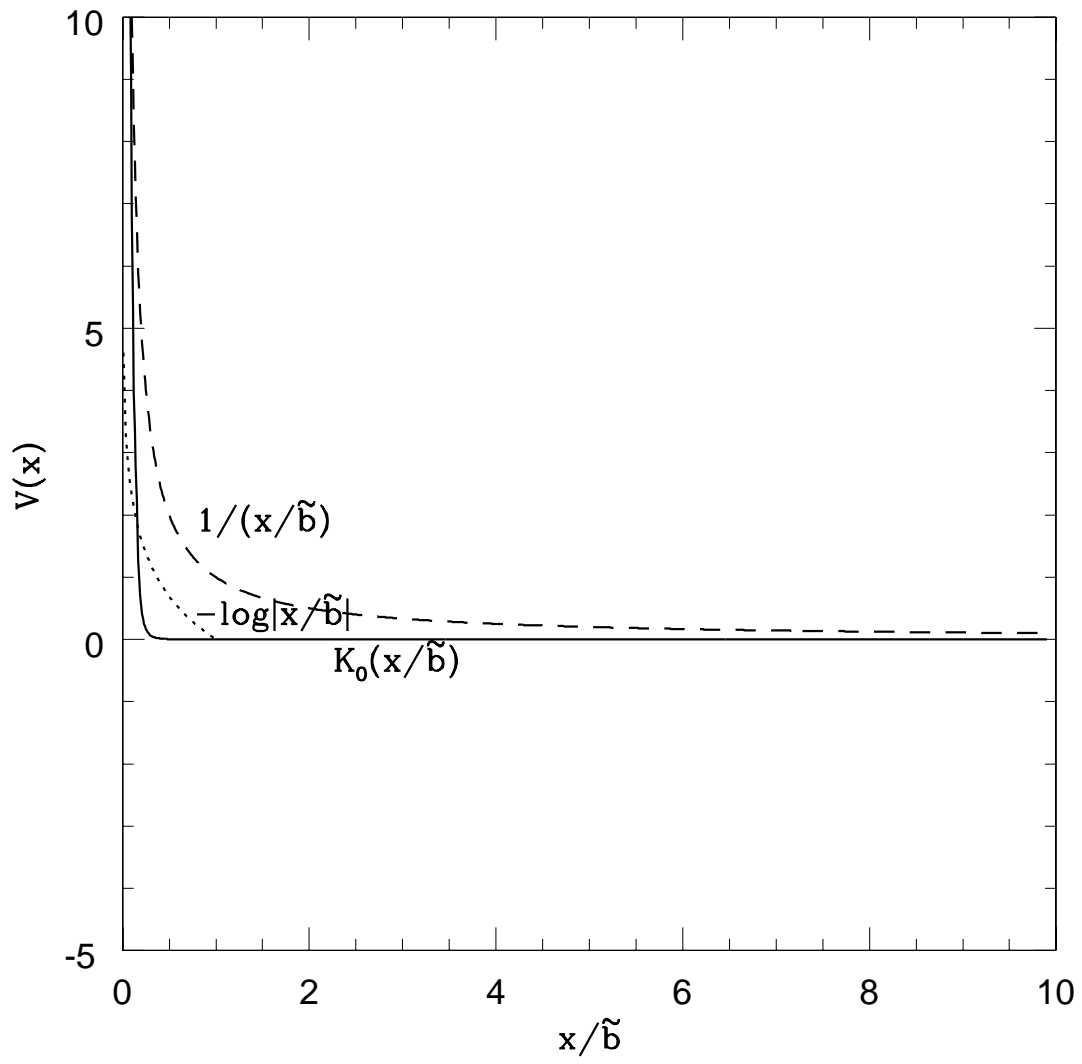


Fig.1, Ghosh et al

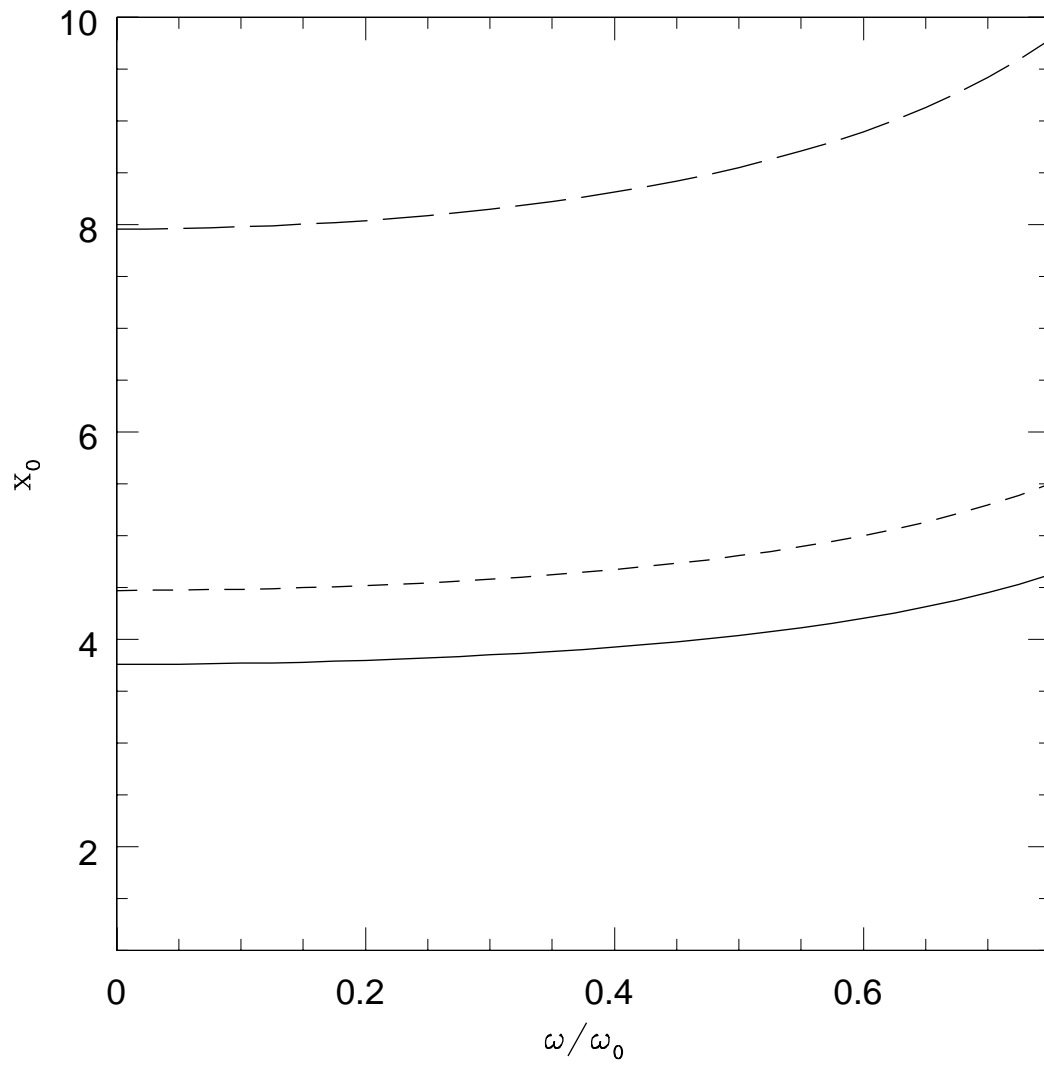


Fig.2, Ghosh et al

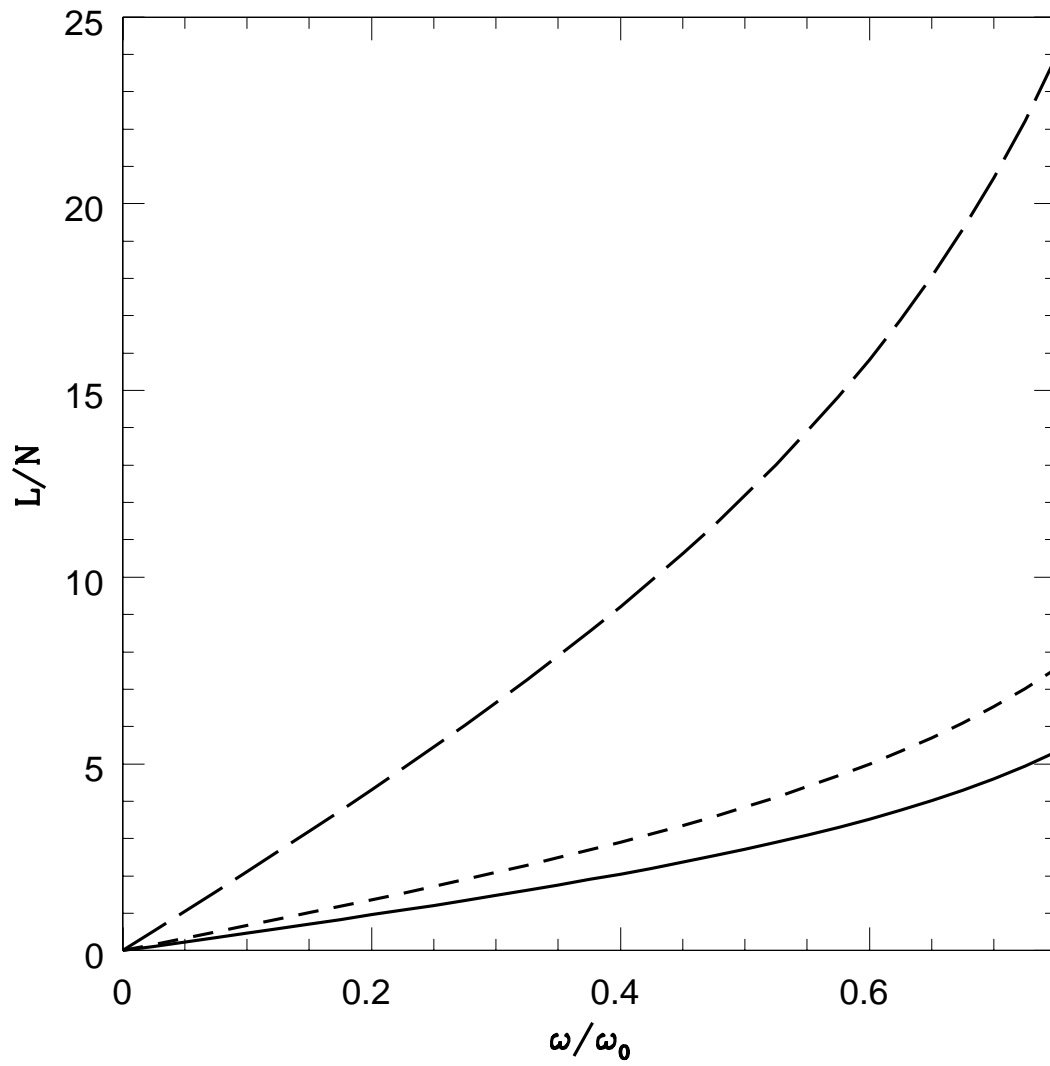


Fig.3, Ghosh et al

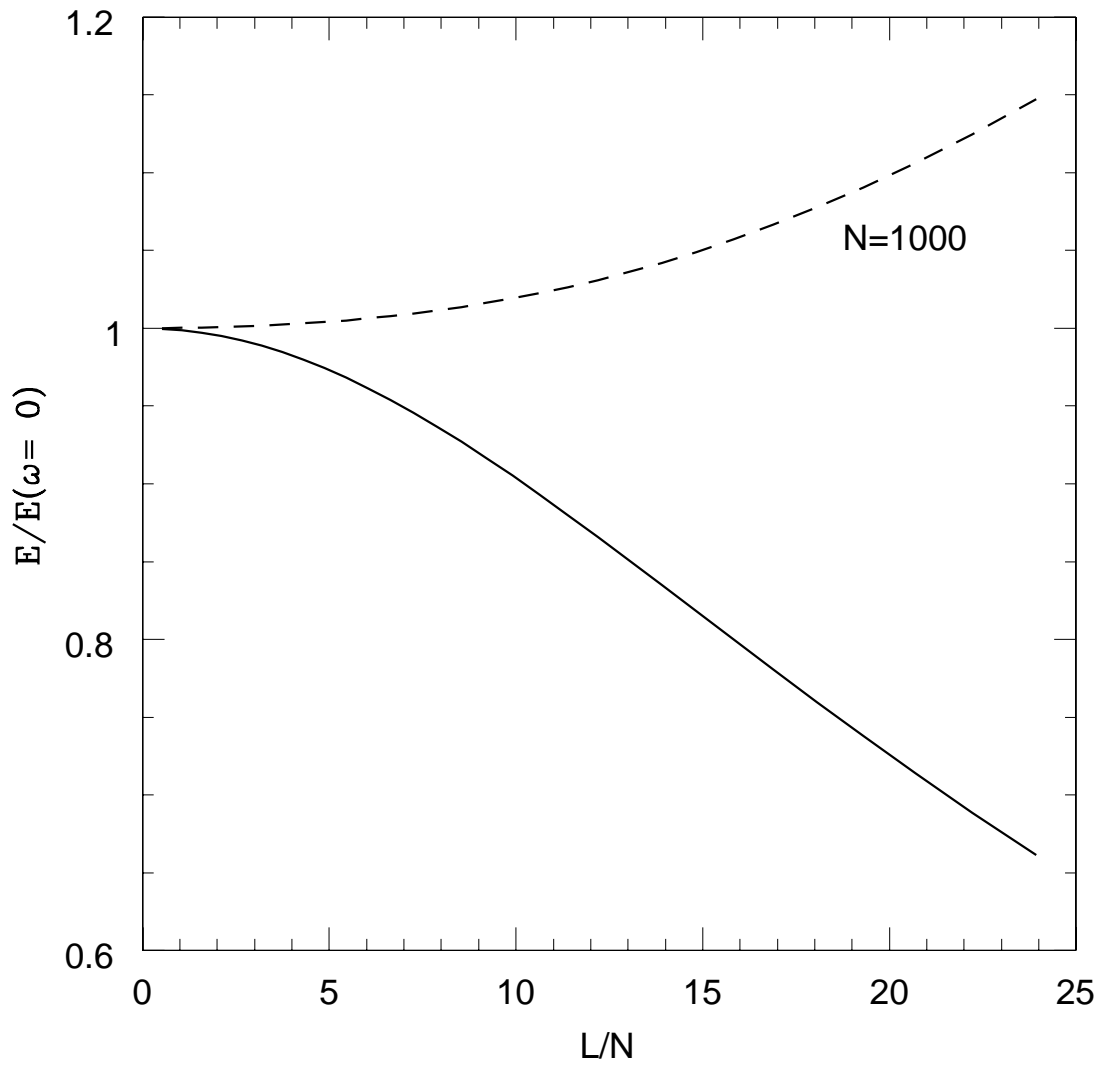


Fig.4, Ghosh et al

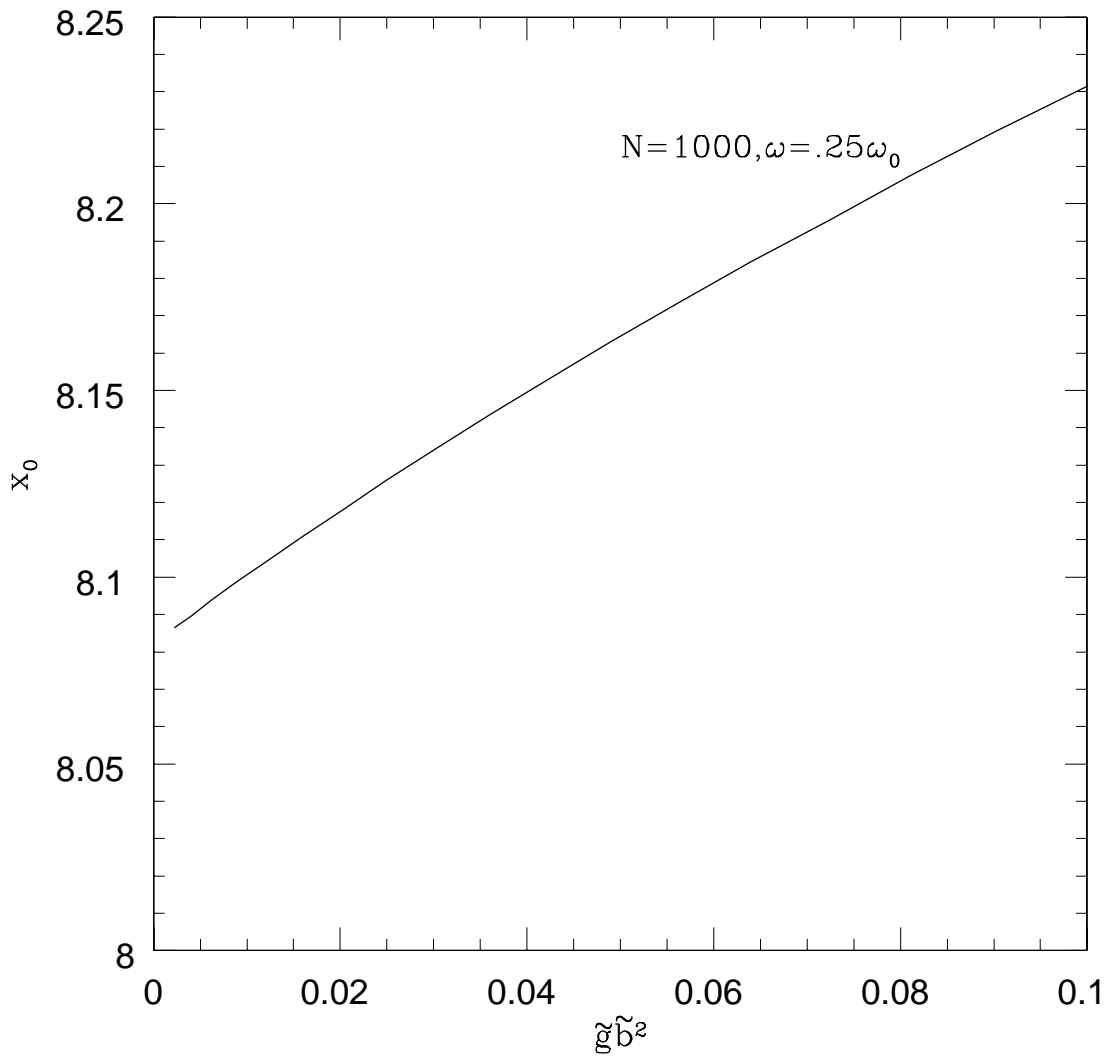


Fig.5, Ghosh et al

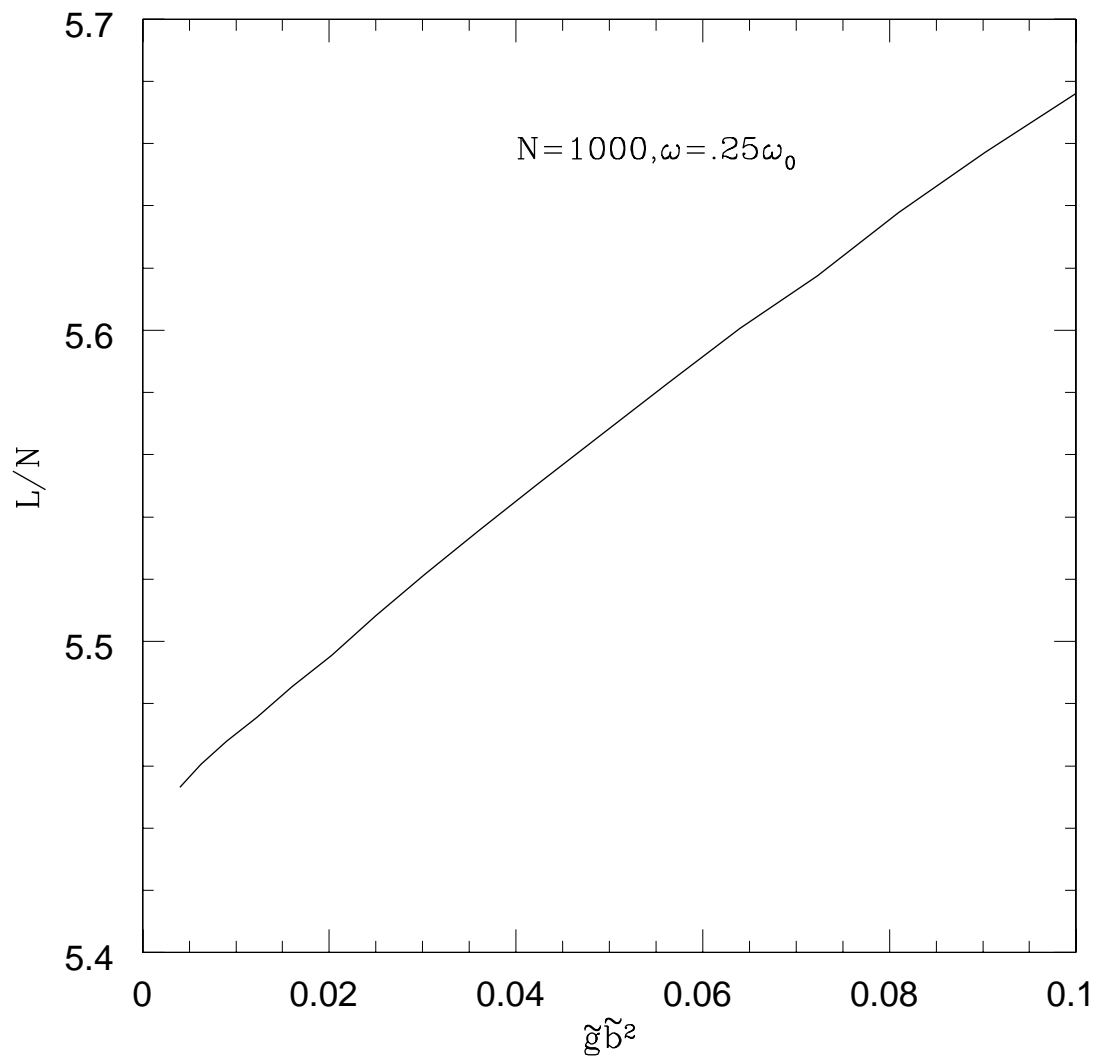


Fig.6, Ghosh et al

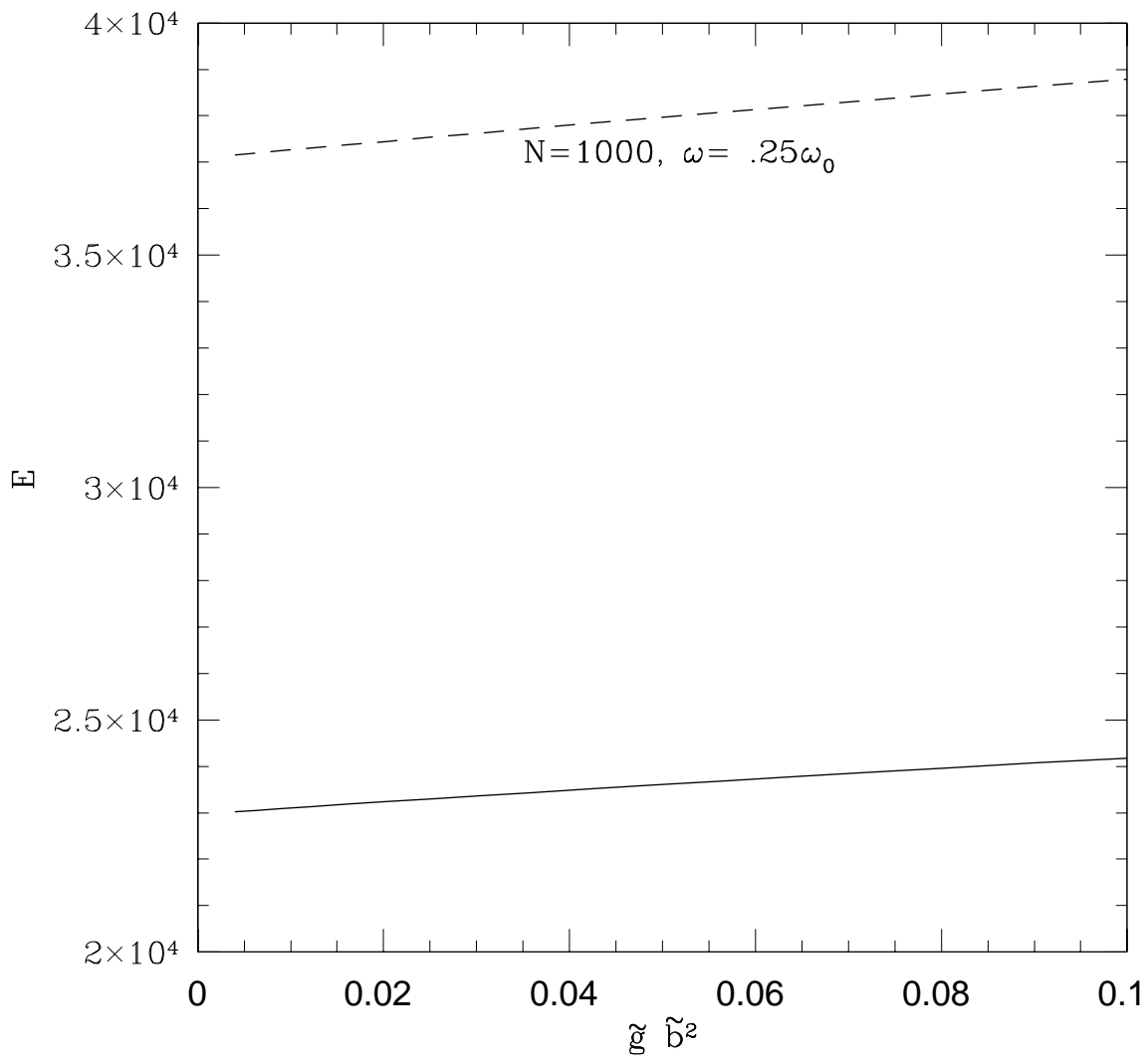


Fig.7, Ghosh et al